Construction of a Risk Score Prognosis Model for Hepatocellular Carcinoma Based on Pyroptosis Related Genes

Xin-yu Li
Shanghai 9th Peoples Hospital Affiliated to Shanghai Jiaotong University School of Medicine
Li-xin Su
Shanghai 9th Peoples Hospital Affiliated to Shanghai Jiaotong University School of Medicine
Ming-zhe Wen
Shanghai 9th Peoples Hospital Affiliated to Shanghai Jiaotong University School of Medicine
Jian-xiong You
Shanghai 9th Peoples Hospital Affiliated to Shanghai Jiaotong University School of Medicine
xi-tao Yang (118120@sh9hospital.org.cn)
Shanghai 9th Peoples Hospital Affiliated to Shanghai Jiaotong University School of Medicine
https://orcid.org/0000-0003-4030-4394

Primary research

Keywords: hepatocellular carcinoma, pyroptosis, overall survival, signature

Posted Date: September 9th, 2021

DOI: https://doi.org/10.21203/rs.3.rs-855956/v1

Abstract

Background: In this study, a prognostic model based on pyroptosis-related genes was established to predict overall survival (OS) in patients with hepatocellular carcinoma(HCC).

Methods: The gene expression data and clinical information of HCC patients were acquired from The Cancer Genome Atlas (TCGA). Using bioinformatics analysis, this predictive signature was constructed and validated. The performance of predictive signature was assessed by the receiver operating characteristic (ROC) curve and the area under the ROC curve (AUC).

Results: A total of 3 pyroptosis-related genes (*BAK1*, *GSDME*, and *NOD2*) were used to construct a survival prognostic model, and experimental validation performed using an experimental cohort. The prognosis model exhibited good performance based on the AUC (AUC: 0.826 at 1 years, 0.796 at 3 years, 0.867 at 5 years). The calibration plots showed excellent calibration.

Conclusion: In this study, a novel prognostic model based on three pyroptosis-related genes is constructed and used to predict the prognosis of HCC patients. The model can accurately and conveniently predict the 1- 3-and 5-year OS of HCC patients.

Introduction

Hepatocellular carcinoma(HCC) is the most common form of liver cancer, accounting for around 90% of the incidence of all liver cancers[1, 2]. China accounts for about half of the total number of new HCC cases and deaths worldwide each year[3]. HCC is associated with high mortality. Prognosis median survival in patients with advanced HCC has been reported to be approximately 6–20 months after diagnosis[4]. Currently, successful available treatments for HCC remain scarce, the main treatment of HCC is surgical resection[5]. The best treatment for patients with advanced HCC remains unclear. The early phase of HCC is generally asymptomatic. HCC is often diagnosed at an advanced stage, when it is often untreatable. The multifactorial etiology of HCC makes prognostic prediction challenging, there is a clear need for the development of novel prognostic models. Pyroptosis is a form of programmed cell death that is highly proinflammatory. Activated caspases cleavage pore-making effect protein Gasdermin D(GSDMD) causing rupture of the plasma membrane, leading to pro-inflammatory cytokine interleukin(IL)-1β and IL-18[6]. The current considerable research have confirmed pyroptosis are potentially effective therapy to cure many malignancies[7–10]. However, whether these genes are correlated with HCC patient prognosis remains largely unknown. In the present study, mRNA expression profiles and corresponding follow-up clinical information were collected from the TCGA database. Then, we constructed a prognostic multigene signature with pyroptosis -related differentially expressed genes (DEGs). In addition,we performed functional enrichment analysis to explore the underlying mechanisms associated with the identified genes.

Materials And Methods

Datasets

Downloaded data RNA-sequencing (RNA-seq) expression data of HCC and corresponding clinical data were downloaded from TCGA. The TCGA cohort was used as a training cohort. Meanwhile, Samples which include gene expression data and corresponding clinical data were collected from 72 human HCC patients from Shanghai Ninth People's Hospital, Shanghai Jiao Tong University School of Medicine. The training cohort included 50 normal human liver samples and 374 HCC samples. Baseline demographic profiles were collected including TNM stage, gender, age, and follow-up(Table 1,Table 2). Then, a total of 52 pyroptosis-related genes from previous systematic reviews were extracted [11, 12].

Identification Of Differentially Expressed Genes

The Bioconductor package edgeR was uesed to normalized read count values of gene expression. Differentially expressed genes (DEGs) analysis performed by limma R package. The criteria of DEGs were as follows: FDR < 0.05 and |log2FC| ≥ 1.

Development And Validation Of The Pyroptosis-related Genes Prognostic Model

Cox regression analysis was performed in order to further assess the prognostic values of the DEGs. In order to ensure accurate results, 0.05 was setted as the cut-off P-value, and 7 survival-related genes were identified for further analysis. In order to avoid overfitting problems, Lasso-penalized Cox regression analysis was performed to develop the best prognostic signature. The penalty parameter(λ) adjustment was performed by tenfold cross-validation based on minimum criteria. Finally, each HCC patient was assigned an individual risk score, and the risk score formula was defined based on the expression level of each gene and the regression coefficient derived from the multivariate Cox regression model. The prognostic signature as risk score = $\sum_{i=1}^{n} exp_i * \beta_i$(Where, *n*, exp_i and β_i, represent the number of prognostic genes, the expression value and the coefficient of gene *i*, respectively). HCC patients were divided into two groups(high-risk and low-risk groups) by a median of risk score. Then, prcomp function in R from the stats package was used to carry out principal component analysys (PCA). PCA was visualized using the ggplot2 R package. In Kaplan–Meier survival analysis, the cut-off value was determined using the function surv_cutpoint of the survival package in R. In addition, a time-dependent receiver operating characteristic (ROC) curve analysis by employing an R package "survivalROC" was plotted to evaluate the predictive accuracy of the gene signature for time-dependent cancer death.

To validate our prognostic model, tumor tissue and normal tissue collected from 72 HCC patients in The First Affiliated Hospital of Zhengzhou University. Using the same risk score formula, the risk score of each patient in the validation cohort was calculated, and patients were classified into the high- or low-risk groups according to the cutoff point of the median risk score. Meanwhile, for the gene which remained

significant in the multivariate Cox analysiswe, we performed real time quantitative PCR (qRT-PCR) and Western Blot. Ethics approval was obtained from the local Ethics Committee of Shanghai Ninth People's Hospital, Shanghai Jiao Tong University School of Medicine.

Quantitative Real-Time PCR

Total RNA was extracted from the target tissue samples and ground thoroughly in a mortar with liquid nitrogen. Each tissue was added to 1 ml Trizol reagent (Life technology, Grand Island, NY, United States) directly to the lysis for 15 min at room temperature on a shaker. To assess the expression level of mRNA, Using parts of total RNA, cDNA was synthesized using the first-strand cDNA synthesis kit (thermo scientific, Lithuania). Quantitative PCR was performed by Roche LightCycler® 480 Real-Time PCR System with SYBR® Green qPCR mix 2.0 kit for measurement. The primers applied in this study are obtained from TsingKe biologicaltechnology (Nanjing,China) including *BAK1* (Forward Primer 5'-GTTTTCCGCAGCTACGTTTTT-3', ReversePrimer 3'-GCAGAGGTAAGGTGACCATCTC-5'), *GSDME* (Forward: 5'-ACATGCAGGTCGAGGAGAAGT-3', Reverse: 3'-TCAATGACACCGTAGGCAATG-5'), *NOD2* (Forward Primer 5'-TGGTTCAGCCTCTCACGATGA-3' Reverse Primer 3'-CAGGACACTCTCGAAGCCTT-5'), *GAPDH*(Forward:5'-ACCCAGAAGACTGTGGATGG-3', Reverse: 5'- CACATTGGGGGTAGGAACA-3'). The relative mRNA levels were calculated by the 2-ΔΔCt method.

Western Blot

A western blot analysis was performed to determine the protein expression of GSDME. The samples were lysed in a RIPA buffer containing protease inhibitors and phosphatase inhibitors. Proteins (40 mg) were separated using SDSPAGE with 10% acrylamide gels. Western blot analysis was performed using antibodies against mouse monoclonal antibody-anti-human GSDME (Cat# ab215191, Abcam), and mouse monoclonal antibody-anti-human bactin (sc-47778, Santa Cruz Biotechnology), followed by incubation with horseradish peroxidase (HRP)-coupled mouse secondary antibody (1:10,000, NA93, GE Healthcare). To confirm equal protein loading, the blots were reprobed with a GAPDH antibody, and analysis of the data was performed using

NIH ImageJ software.

Functional enrichment analysis

Kyoto Encyclopedia of Genes and Genomes (KEGG) and Gene Ontology (GO) enrichment analyses of DEGs were performed by using the “clusterProfiler” R package, The infiltrating score of 16 immune cells and the activity of 13 immune-related pathways were calculated using the single-sample gene set enrichment analysis (ssGSEA) method in the Gene Set Variation Analysis (GSVA) package of R software. Meanwhile,we analyzed the correlation of 3 pyroptosis-related DEGs expression with infiltrating immune cells with the help of ssGSEA. *SIGLEC15, IDO1, CD274, HAVCR2, PDCD1, CTLA4, LAG3*, and *PDCD1LG2* were selected to be immune-checkpoint–relevant transcripts and the expression values of these eight genes were extracted. All the above analysis methods and R package were implemented by R foundation for statistical computing (2020) version 4.0.3 and software packages ggplot2 and pheatmap.

Results

Identification of prognostic pyroptosis-related DEGs and Construction of a prognostic model

A total of 50 normal tissue samples and 374 tumor tissue samples of HCC were screened from the TCGA database. Table 1 shows the clinicopathological data of the patients with HCC included in the study. A total of 30 differential genes(DEGs) were identified between tumor and the adjacent nontumor tissues. The DEGs expression in tumor and the adjacent nontumor tissues was represented in the heatmap(Fig. 1a,green: low expression level;red:high expression level). Also, The relationship between these genes is presented in Fig. 1b,which suggesting the tight relationship between these genes.

The prognostic values of DEGs were evaluated by univariate Cox analysis, and 7 genes that were significantly related to the OS of patients were identified(Fig. 1c). To build a prognostic model for HCC, we used training dataset and applied the LASSO Cox regression analysis to identify stable markers from 7-survival-related genes mentioned above. To find an optimal λ, 10-fold cross validation with minimum criteria was employed, so the final model gave minimum cross validation error. Then, 3 DEGs(*BAK1*, *GSDME*, and *NOD2*)were identified(Fig. 2a-2b). Using the following formula, the risk score was calculated 0.045673* expression level of *BAK1* + 0.005602* expression level of *NOD2* + 0.143950* expression level of *GSDME*. A median cut-off value was applied to stratify patients into a high-risk group (n = 183) and a low-risk group (n = 182)(Fig. 3a). The PCA showed that patients in different risk groups were distributed in two directions by the constructed model cohort (Fig. 3b). In the high risk score group, the risk of mortality obviously increased with the risk score increased (Fig. 3c). Kaplan-Meier analysis showed that the probability of survival was significantly higher in low-risk patients than in high-risk patients(Fig. 3d,$p < 0.05$). The calibration plots showed that calibration appeared good between the predicted and observed risks(Fig. 3e). Also, the AUC of the time-dependent ROC curve was plotted to assess the prognostic effect. the AUC of the prognostic risk assessment model was 0.844 at 1 years, 0.889 at 3 years, 0.774 at 5 years (Fig. 3f).

Validation Of The 3-gene Prognostic Model

In order to evaluate the robustness of the prognostic model constructed using data from the training cohort, its performance was also assessed using validation cohort. The risk score for each patient in validation cohort was calculated with the same formula as training group. The AUC of the 3-gene signature was 0.787 at 1 years, 0.801 at 3 years, 0.820 at 5 years(Fig. 4a). Besides, patients in the high-risk group were significantly worse off the overall survival time compared to the low-risk group (Fig. 4b). Western Blot and qRT-PCR was used to detect *GSDME* expression. The results showed that *GSDME* expression in HCC was significantly higher than that in adjacent tissues(Fig. 5).

Independent Prognostic Value Of The Risk Model

To investigate the prognostic value of different clinical features in HCC, univariate Cox regression analysis was performed. According to the results of univariate Cox regression analysis, the risk model showed their prognostic value in predicting OS(Fig. 6a). The multivariable Cox regression analysis suggested risk score had prognostic value for HCC patients. Even after adjusting for confounding factors, the risk score is still a prognostic factor(Fig. 6b) for patients with HCC. Figure 6c shows heatmaps of the pyroptosis-related DEGs modules on the clinical data and found a different distribution of patients' age and survival status between low- and high-risk subgroups.

DEGs-based tumor classification.

In addition, We explore the connections between the expression of DEGs and HCC subtypes, consensus clustering analysis was used to classify HCC patients into subtypes. By increasing the clustering variable (k) from 2 to 10, we found that the highest intra-group correlation and low inter-group correlation was observed when k = 2 (Fig. 7a). The results showed that the HCC patients could be well divided into two clusters based on the DEGs.The gene expression profile were matched to the clinical data and was presented in a heatmap (Fig. 7b), We also compared the OS in 2 clusters.There were significant differences in 2 clusters (Fig. 7c).

Functional Analyses And Infiltrating Immune Cells

Meanwhile, GO function and KEGG pathway enrichment analysis were used to investigate the intrinsic pathway of DEGs. GO function analysis was performed using three ontologies: biological process (BP), cellular component (CC), and molecular function (MF). Based on GO analysis, the DEGs were most enriched in BP, and specifically in immune related processes(such as T cell activation, regulation of T cell activation, leukocyte cell – cell adhesion, Fig. 8a). In addition, KEGG pathway analyses indicated that these DEGs were highly enriched in Cytokine – cytokine receptor interaction, Neuroactive ligand – receptor interaction, Chemokine signaling pathway(Fig. 8b). To further explore relationship between immune cell infiltration and risk scores in the prognostic risk mode, ssGSEA score was used to quantify the level of enrichment of immune cell functions or pathways in cancer samples(Fig. 9a-b). One interesting finding is the many types of immune cells were significantly different between the two groups(such as macrophages, activated dendritic cell, Treg). Another intriguing fact was the immune cell functions were also significantly different between the two groups(such as APC_co_inhibition, CCR, Check – point, HLA, MHC_class_I, Type_II_IFN_Reponse). There are also significant differences in immune checkpoint-related genes in patients of different grades(Fig. 9c).

Discussion

Worldwide, liver cancer is the fourth most common cause of cancer-related death, with the sixth highest incidence rate[13]. HCC accounts for 70–85% of primary liver cancer cases and is an important medical

problem [14, 15]. If caught in time, HCC can be cured by surgery or liver transplantation, but patients in the early stages of HCC are generally asymptomatic, tumors grow rapidly during this period [16]. Many HCC patients are diagnosed at intermediate or late stages, only 20–30% of HCC are detected at an early stage [17, 18]. As treatment modalities are limited and the high mortality rates of HCC[19], the prognostic evaluation of HCC patients is very important. Pyroptosis is a newly identified type of programmed cell death that is different from apoptosis and necrosis and can be initiated in response to various intracellular or extracellular stimuli. Pyroptosis is mainly mediated by Caspase-1/3/4/5/11 and Gasdermin family, and characterized by cell swelling,membrane lysis and release of proinflammatory factors.

In this study, we constructed a prognostic score model of a 3-gene signature(*BAK1, GSDME*, and *NOD2*) for predicting the prognosis of HCC. with the help of Lasso-penalized Cox regression, the model showed good results by its ability to predict OS for HCC(AUC: 0.844 at 1 years, 0.889 at 3 years, 0.774 at 5 years in training group). Combining our own collected and sequenced samples, it attest to the fact that the 3-gene signature is useful tools(AUC: 0.787 at 1 years, 0.801 at 3 years, 0.820 at 5 years in validation group). The calibration plots showed excellent agreement.

Previous related researchs study arrived at similar conclusions to our own. *BAK1* is an important regulator of ferroptosis in the *BCL2* family. Up-regulation of *BAK1* gene expression can affect the volume of HCC tumors[20]. Intracellular *GSDME* level is an important determinant of the type of cell death[21, 22]. The high expression of *GSDME* determines that tumour cell undergo ferroptosis rather than apoptosis, suggesting that the combination of methylation enzyme inhibitors and antitumour agents may be more effective in killing tumour cells. *GSDME* expression levels regulate the apoptosis- ferroptosis transition and play an important role in the treatment of a variety of tumours[23, 24]. *NOD2* can play an important role in the development of inflammation-associated tumours by activating transcription factors such as NF-κB and STAT1. NF-κB is a nuclear protein factor with pleiotropic regulatory effects, involved in pathophysiological processes such as oxidative stress, inflammation and cell proliferation in the body, and when activated, activates effector caspase-3, which is involved in regulating the transcription of pyroptosis genes, ultimately leading to DNA strand breakage and pyroptosis.

During the past few years, the role of the pyroptosis in tumor susceptibility has become an intense area of research, the potential roles of pyroptosis in the tumor immune remain elusive[25]. Based on the significant results of the GO enrichment analysis, there were immune-related biological processes and pathways were enriched which suggests a surprisingly close association with tumor immunity. From this, it can be inferred that pyroptosis with tumor immune have a close relationship. Pyroptosis may have affected progress of the tumor through immune mechanisms. Macrophages, activated dendritic cell, Treg were significantly different between the two groups. Previous studies have demonstrated that parainflammation, a low-grade form of inflammation, is widely prevalent in human cancer. Therefore, widespread parainflammation can explain the enrichment of many immune-related biological processes in HCC patients. Previous studies have confirmed that Treg cells are important immunosuppressive cells

in malignant tumours[26]. A new subpopulation of macrophages, called Podoplanin-expressing macrophages (PoEMs), has also been identified, which can alter tissues in the vicinity of tumours, thereby promoting the spread of cancer cells[27]. Immune cheeckpoint are regulatory molecules that play an inhibitory role in the immune system and are essential for maintaining self-tolerance, preventing autoimmune responses, and minimizing tissue damage by controlling the duration and intensity of the immune response[28]. Expression of immune cheeckpoint on immune cells will inhibit the function of immune cells and prevent the body from producing an effective anti-tumor immune response, and the tumor will form an immune escape. On the basis of our results, there was significant difference in immune cheeckpoint between patients with different HCC stages. Previous studies have confirmed Treg was important immune suppressor cells that play a suppressive function in the immune system. Tumor cells can use immune checkpoints to escape immune cell attacks.

Conclusion

In summary, we developed a novel prognostic model based on 3 pyroptosis related genes and used it to predict the prognosis risk of in HCC patients. This model proved to be significantly associated with the OS in both the derivation and validation cohorts, which might provide insight into the prediction of HCC prognosis.

Declarations

Acknowledgements Home for Researchers editorial team（www.home-for-researchers.com）

Availability of data and materials: For availability of data and materials, please contact author for data request.

Financial Support: This study received Fundamental research program funding of Ninth People's Hospital affiliated to Shanghai Jiao Tong university School of Medicine (No. JYZZ076), Clinical Research Program of Ninth People's Hospital, Shanghai Jiao Tong University School of Medicine (No. JYLJ201801, JYLJ201911), the China Postdoctoral Science Foundation (No. 2017M611585) and the National Natural Science Foundation of China (No. 81871458).

Competing interests: no conflicts of interest.

Contributors: Xi-tao Yang, Li-xin Su designed experiments;Ming-zhe Weng, Jian-xiong You,Xin-yu Li , carried out experiments, and wrote the manuscript, Xi-tao Yang, Li-xin Su performed manuscript review.

Patient consent: Obtained.

Ethics approval: All procedures performed in the studies involving human participants were in accordance with the Scientific Research Projects Approval Determination of Independent Ethics Committee of

Shanghai Ninth People's Hospital, Shanghai Jiao Tong University School of Medicine, with the 1964 Helsinki Declaration and its later amendments or comparable ethical standards.

Category: original article

References

1. Zhang Q, He Y, Luo N, et al. Landscape and Dynamics of Single Immune Cells in Hepatocellular Carcinoma.[J]. Cell,2019,179(4):829-845.DOI:10.1016/j.cell.2019.10.003
2. Lin H, Hua F, Hu Z. Autophagic flux, supported by toll-like receptor 2 activity, defends against the carcinogenesis of hepatocellular carcinoma.[J]. Autophagy,2012,8(12):1859-1861.DOI:10.4161/auto.22094
3. Kulik L, El-Serag H B. Epidemiology and Management of Hepatocellular Carcinoma[J]. Gastroenterology,2019,156(2):477-491.DOI:10.1053/j.gastro.2018.08.065
4. Wu D, Yang X, Peng H, et al. OCIAD2 suppressed tumor growth and invasion via AKT pathway in Hepatocelluar carcinoma[J]. Carcinogenesis,2017,38(9):910-919.DOI:10.1093/carcin/bgx073
5. Chen C, Chen C, Shieh T, et al. Corylin Suppresses Hepatocellular Carcinoma Progression via the Inhibition of Epithelial-Mesenchymal Transition, Mediated by Long Noncoding RNA GAS5[J]. International journal of molecular sciences,2018,19(2):380.DOI:10.3390/ijms19020380
6. Shi J, Gao W, Shao F. Pyroptosis: Gasdermin-Mediated Programmed Necrotic Cell Death.[J]. Trends in biochemical sciences,2017,42(4):245-254.DOI:10.1016/j.tibs.2016.10.004
7. Liu Y, Guo F, Guo W, et al. Ferroptosis-related genes are potential prognostic molecular markers for patients with colorectal cancer.[J]. Clinical and experimental medicine,2021.DOI:10.1007/s10238-021-00697-w
8. Yang Y, Liu T, Hu C, et al. Ferroptosis inducer erastin downregulates androgen receptor and its splice variants in castration-resistant prostate cancer.[J]. Oncology reports,2021,45(4).DOI:10.3892/or.2021.7976
9. Jiao Y, Zhao H, Chen G, et al. Pyroptosis of MCF7 Cells Induced by the Secreted Factors of hUCMSCs.[J]. Stem cells international,2018,2018:5912194.DOI:10.1155/2018/5912194
10. Gao J, Qiu X, Xi G, et al. Downregulation of GSDMD attenuates tumor proliferation via the intrinsic mitochondrial apoptotic pathway and inhibition of EGFR/Akt signaling and predicts a good prognosis in non-small cell lung cancer.[J]. Oncology reports,2018,40(4):1971-1984.DOI:10.3892/or.2018.6634
11. Karki R, Kanneganti T. Diverging inflammasome signals in tumorigenesis and potential targeting.[J]. Nature reviews. Cancer,2019,19(4):197-214.DOI:10.1038/s41568-019-0123-y
12. Xia X, Wang X, Cheng Z, et al. The role of pyroptosis in cancer: pro-cancer or pro-"host"?[J]. Cell death & disease,2019,10(9):650.DOI:10.1038/s41419-019-1883-8

13. Villanueva A. Hepatocellular Carcinoma.[J]. The New England journal of medicine,2019,380(15):1450-1462.DOI:10.1056/NEJMra1713263
14. Feng Y, Feng C, Chen S, et al. Cyproheptadine, an antihistaminic drug, inhibits proliferation of hepatocellular carcinoma cells by blocking cell cycle progression through the activation of P38 MAP kinase.[J]. BMC cancer,2015,15:134.DOI:10.1186/s12885-015-1137-9
15. Forner A, Reig M, Bruix J. Hepatocellular carcinoma.[J]. Lancet (London, England),2018,391(10127):1301-1314.DOI:10.1016/S0140-6736(18)30010-2
16. Sengupta B, Siddiqi S A. Hepatocellular carcinoma: important biomarkers and their significance in molecular diagnostics and therapy.[J]. Current medicinal chemistry,2012,19(22):3722-3729
17. CIRSE 2008. Abstracts of the annual meeting of the Cardiovascular and Interventional Radiological Society of Europe. September 13-17, 2008. Copenhagen, Denmark.[J]. Cardiovascular and interventional radiology,2008,31 Suppl 3(Suppl 3):237-521.DOI:10.1007/s00270-008-9395-4
18. Scudellari M. Drug development: try and try again.[J]. Nature,2014,516(7529):S4-S6.DOI:10.1038/516S4a
19. Baglieri J, Brenner D A, Kisseleva T. The Role of Fibrosis and Liver-Associated Fibroblasts in the Pathogenesis of Hepatocellular Carcinoma.[J]. International journal of molecular sciences,2019,20(7).DOI:10.3390/ijms20071723
20. Chen W, Quan Y, Fan S, et al. Exosome-transmitted circular RNA hsa_circ_0051443 suppresses hepatocellular carcinoma progression.[J]. Cancer letters,2020,475:119-128.DOI:10.1016/j.canlet.2020.01.022
21. Wang Y, Gao W, Shi X, et al. Chemotherapy drugs induce pyroptosis through caspase-3 cleavage of a gasdermin.[J]. Nature,2017,547(7661):99-103.DOI:10.1038/nature22393
22. Rogers C, Fernandes-Alnemri T, Mayes L, et al. Cleavage of DFNA5 by caspase-3 during apoptosis mediates progression to secondary necrotic/pyroptotic cell death.[J]. Nature communications,2017,8:14128.DOI:10.1038/ncomms14128
23. Lu H, Zhang S, Wu J, et al. Molecular Targeted Therapies Elicit Concurrent Apoptotic and GSDME-Dependent Pyroptotic Tumor Cell Death.[J]. Clinical cancer research : an official journal of the American Association for Cancer Research,2018,24(23):6066-6077.DOI:10.1158/1078-0432.CCR-18-1478
24. Kim M S, Lebron C, Nagpal J K, et al. Methylation of the DFNA5 increases risk of lymph node metastasis in human breast cancer.[J]. Biochemical and biophysical research communications,2008,370(1):38-43.DOI:10.1016/j.bbrc.2008.03.026
25. Banerjee T, Calvi L M, Becker M W, et al. Flaming and fanning: The Spectrum of inflammatory influences in myelodysplastic syndromes.[J]. Blood reviews,2019,36:57-69.DOI:10.1016/j.blre.2019.04.004
26. Wang L, Simons D L, Lu X, et al. Connecting blood and intratumoral T(reg) cell activity in predicting future relapse in breast cancer.[J]. Nature immunology,2019,20(9):1220-1230.DOI:10.1038/s41590-019-0429-7

27. Bieniasz-Krzywiec P, Martín-Pérez R, Ehling M, et al. Podoplanin-Expressing Macrophages Promote Lymphangiogenesis and Lymphoinvasion in Breast Cancer.[J]. Cell metabolism,2019,30(5):917-936.DOI:10.1016/j.cmet.2019.07.015
28. Ravi R, Noonan K A, Pham V, et al. Bifunctional immune checkpoint-targeted antibody-ligand traps that simultaneously disable TGFβ enhance the efficacy of cancer immunotherapy[J]. Nature communications,2018,9(1):741.DOI:10.1038/s41467-017-02696-6

Tables

Table1. Clinical characteristics of the HCC patients used in the derivation cohort

Characteristic	levels	Overall
n		374
T stage, n (%)	T1	183 (49.3%)
	T2	95 (25.6%)
	T3	80 (21.6%)
	T4	13 (3.5%)
N stage, n (%)	N0	254 (98.4%)
	N1	4 (1.6%)
M stage, n (%)	M0	268 (98.5%)
	M1	4 (1.5%)
Pathologic stage, n (%)	Stage I	173 (49.4%)
	Stage II	87 (24.9%)
	Stage III	85 (24.3%)
	Stage IV	5 (1.4%)
Gender, n (%)	Female	121 (32.4%)
	Male	253 (67.6%)
Age, n (%)	<=60	177 (47.5%)
	>60	196 (52.5%)
Histologic grade, n (%)	G1	55 (14.9%)
	G2	178 (48.2%)
	G3	124 (33.6%)
	G4	12 (3.3%)
OS event, n (%)	Alive	244 (65.2%)
	Dead	130 (34.8%)
Age, median (IQR)		61 (52, 69)

Table 2. Clinical characteristics of the HCC patients used in the validation cohort

Characteristic	levels	Overall
n		72
Age, n (%)	<=60	40 (55%)
	>60	32 (45%)
Gender, n (%)	Female	27 (36%)
	Male	45 (64%)
T stage, n (%)	T1	22 (30%)
	T2	18 (25%)
	T3	18 (25%)
	T4	14 (20%)
N stage, n (%)	N0	68(95%)
	N1	4 (5%)
M stage, n (%)	M0	70(97%)
	M1	2 (3%)
Pathologic stage, n (%)	Stage I	36(50%)
	Stage II	18 (25%)
	Stage III	14 (20%)
	Stage IV	4 (5%)
Histologic grade, n (%)	G1	9(12%)
	G2	35(48%)
	G3	25(35%)
	G4	3 (4%)
Age, median (IQR)		61.5 (51, 74.25)

Figures

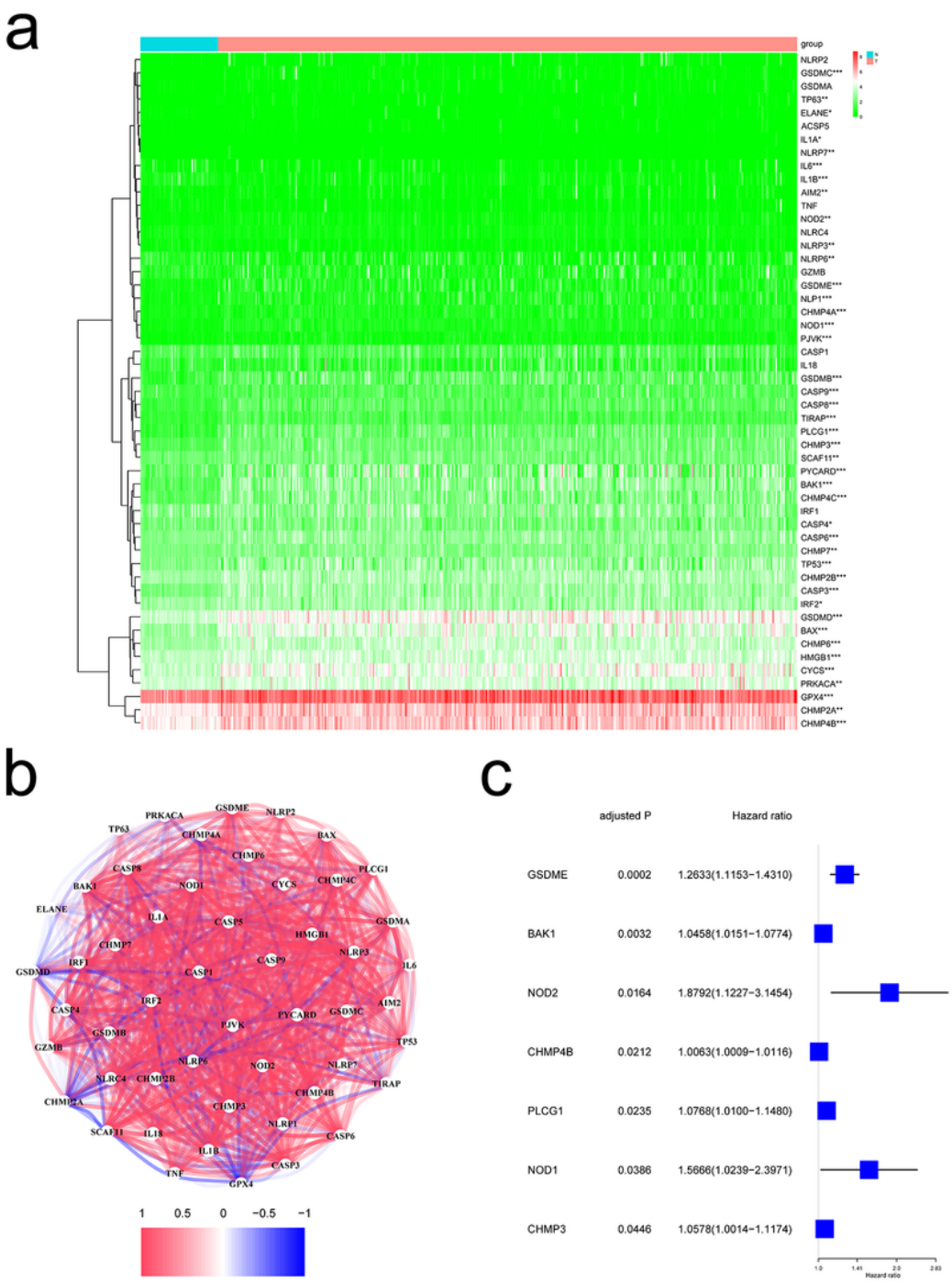

Figure 1

Identification of the candidate genes.a. Heatmap of the differential gene expression in the two groups. b. The relationship between these genes.c. Forest plots showing the results of the univariate Cox regression analysis between gene expression and OS.

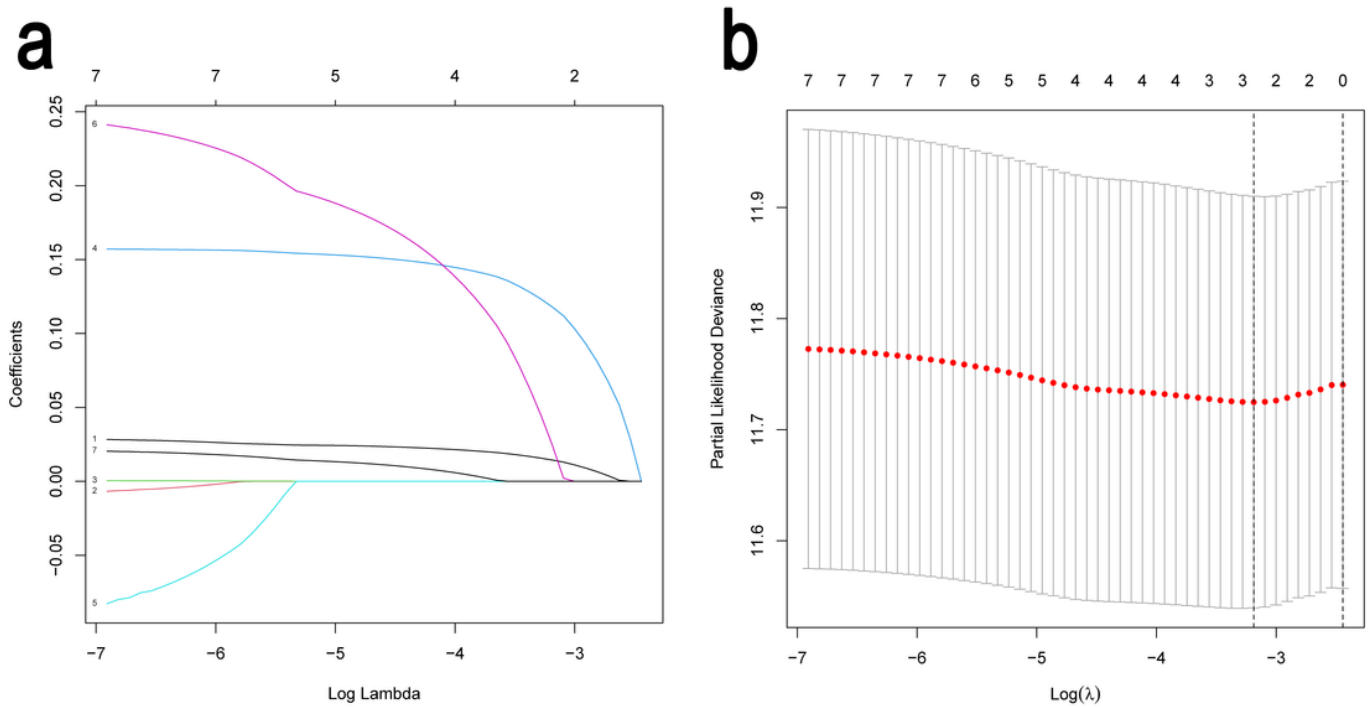

Figure 2

Processes of LASSO Cox model fitting. a. The profile of coefficients in the model at varying levels of penalization plotted against the log (lambda) sequence. b. Tenfold cross-validated error (first vertical line equals the minimum error, whereas the second vertical line shows the cross-validated error within 1 standard error of the minimum) .

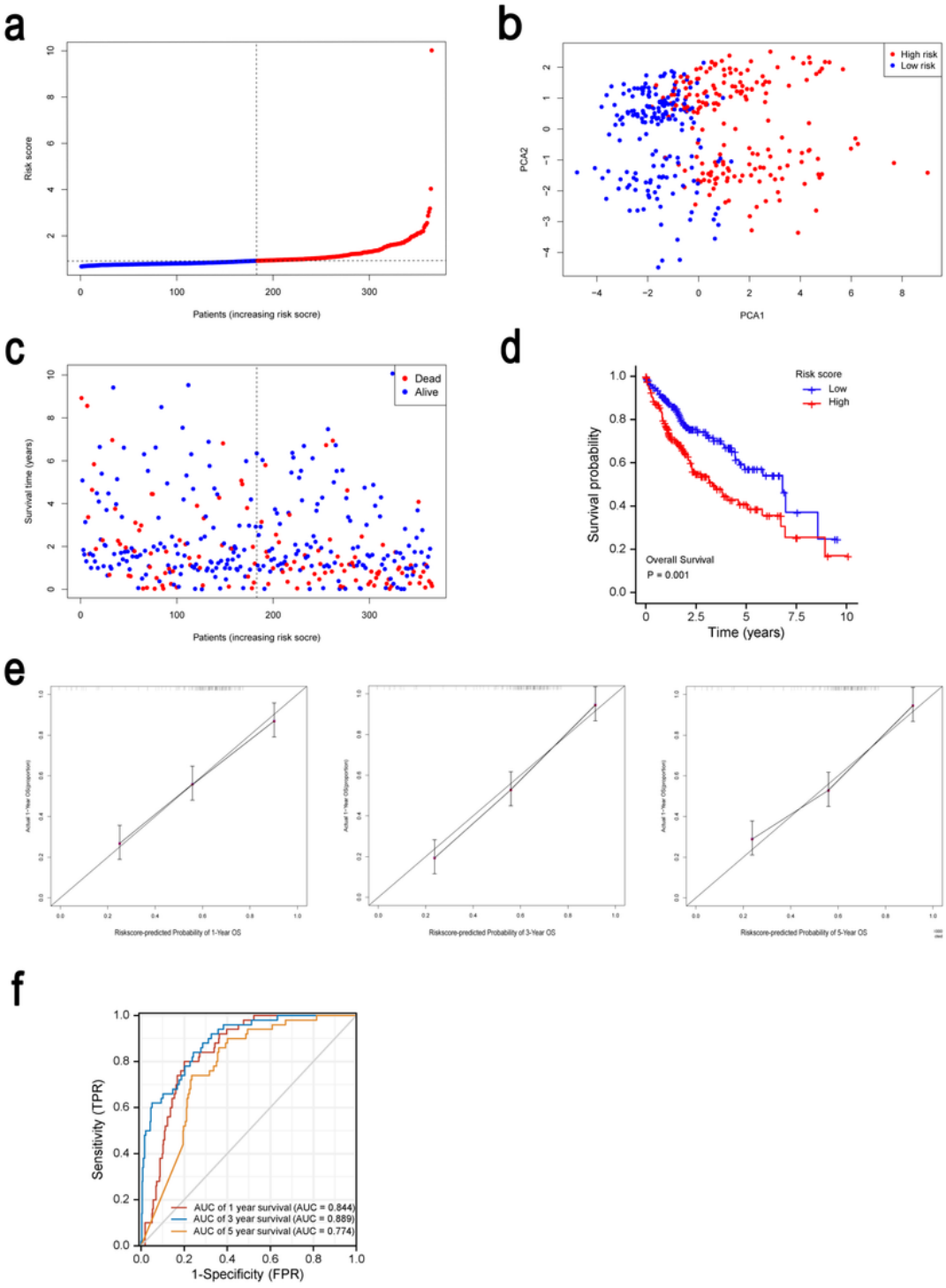

Figure 3

Prognostic analysis of the 3-gene signature model in the derivation cohort. a. The distribution and median value of the risk scores in the derivation cohort.b. PCA plot of the derivation cohort.c. The distributions of OS status, OS and risk score in the derivation cohort.d. Kaplan-Meier curves for the OS of patients in the high-risk group and low-risk group in the derivation cohort. e. Calibration plot for model. f.

AUC of time-dependent ROC curves verified the prognostic performance of the risk score in the derivation cohort.

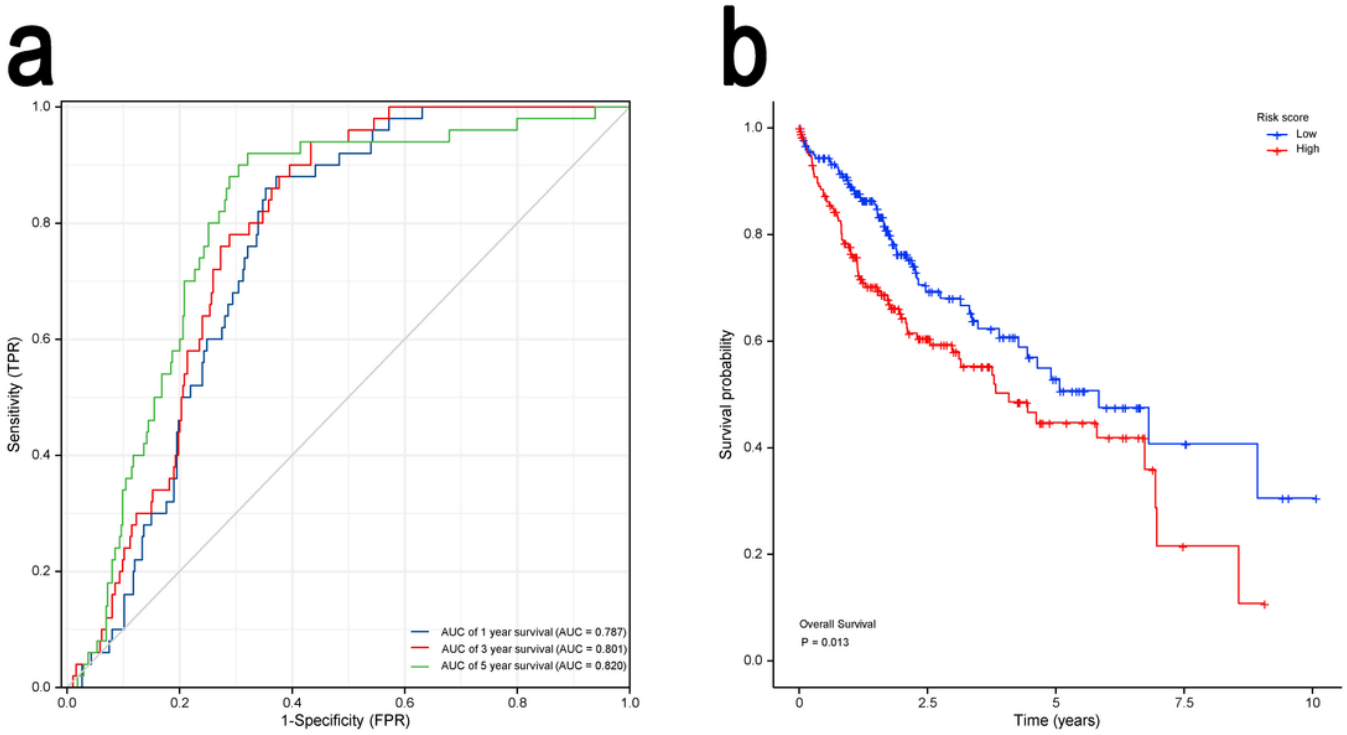

Figure 4

Validation of the 3-gene signature in the validation cohort. a. AUC of time-dependent ROC curves verified the prognostic performance of the risk score in the validation cohort. b. Kaplan-Meier curves for the OS of patients in the high-risk group and low-risk group in the validation cohort.

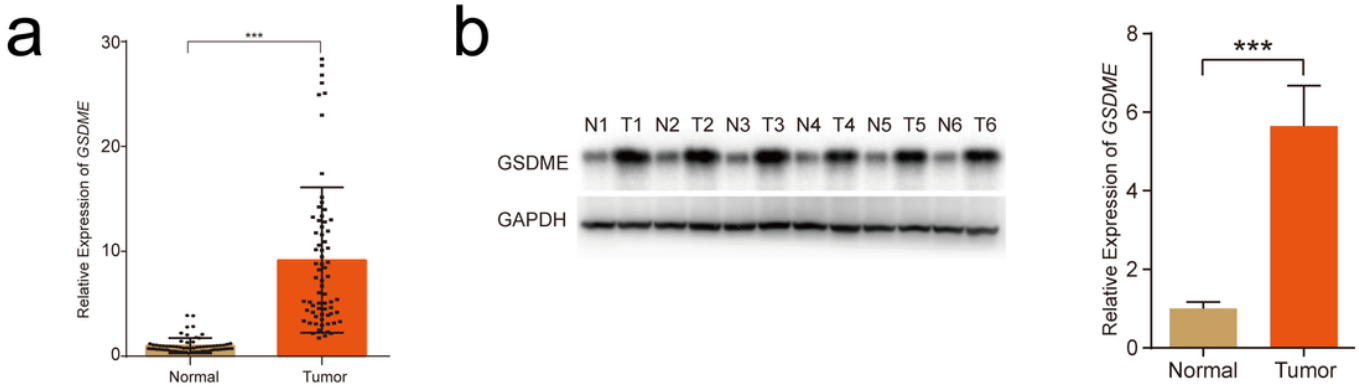

Figure 5

Quantitative real-time PCR (qRT-PCR) and western blotting a. Results of qRT-PCR analysis. b. Western blot analysis showed a clear overexpression in protein expression levels of GSDME in HCC.

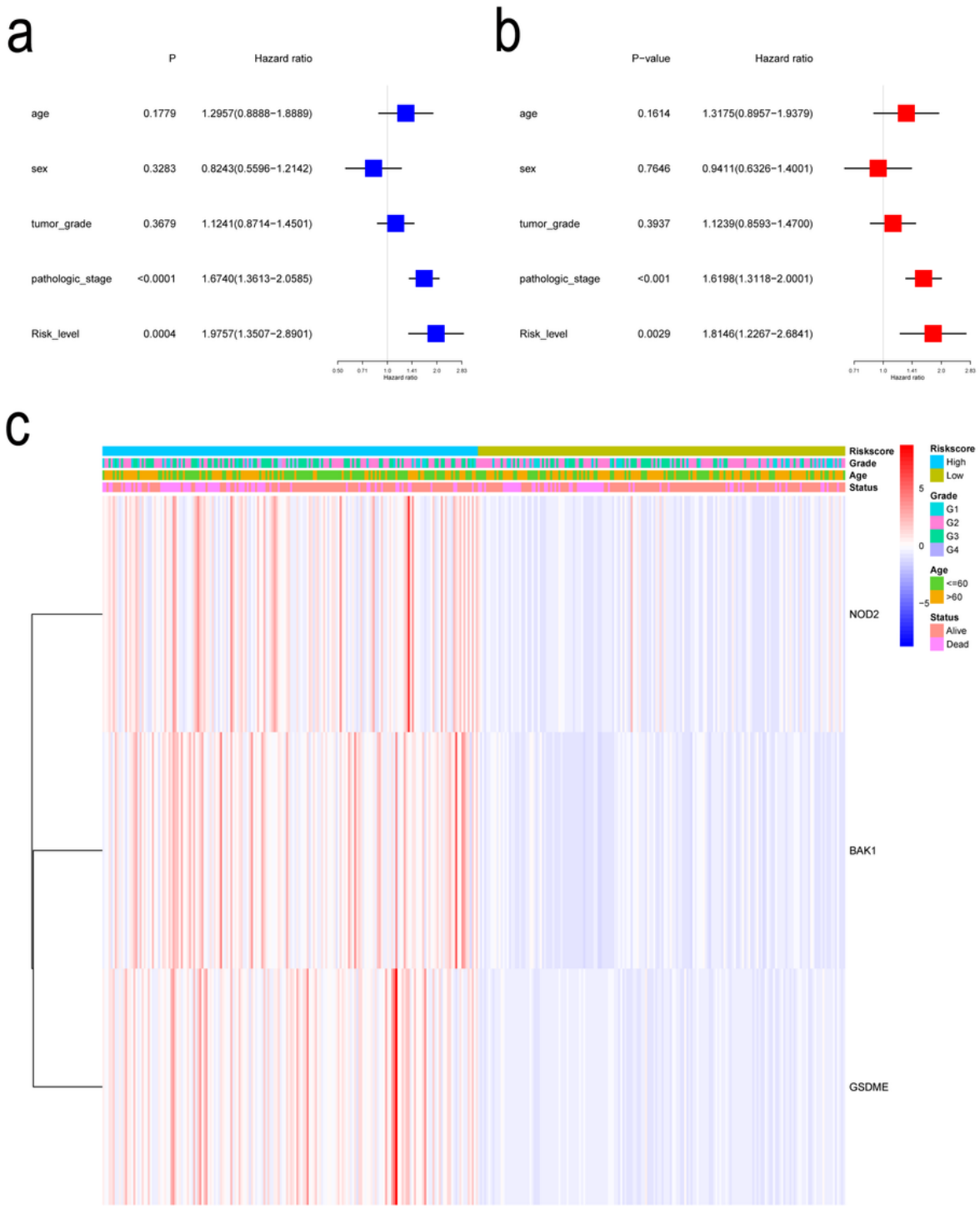

Figure 6

a-b Univariate and multivariate Cox regression outcome (Hazard Ratios 95% CI) .c. Heatmap for the connections between clinicopathologic features and the risk groups.

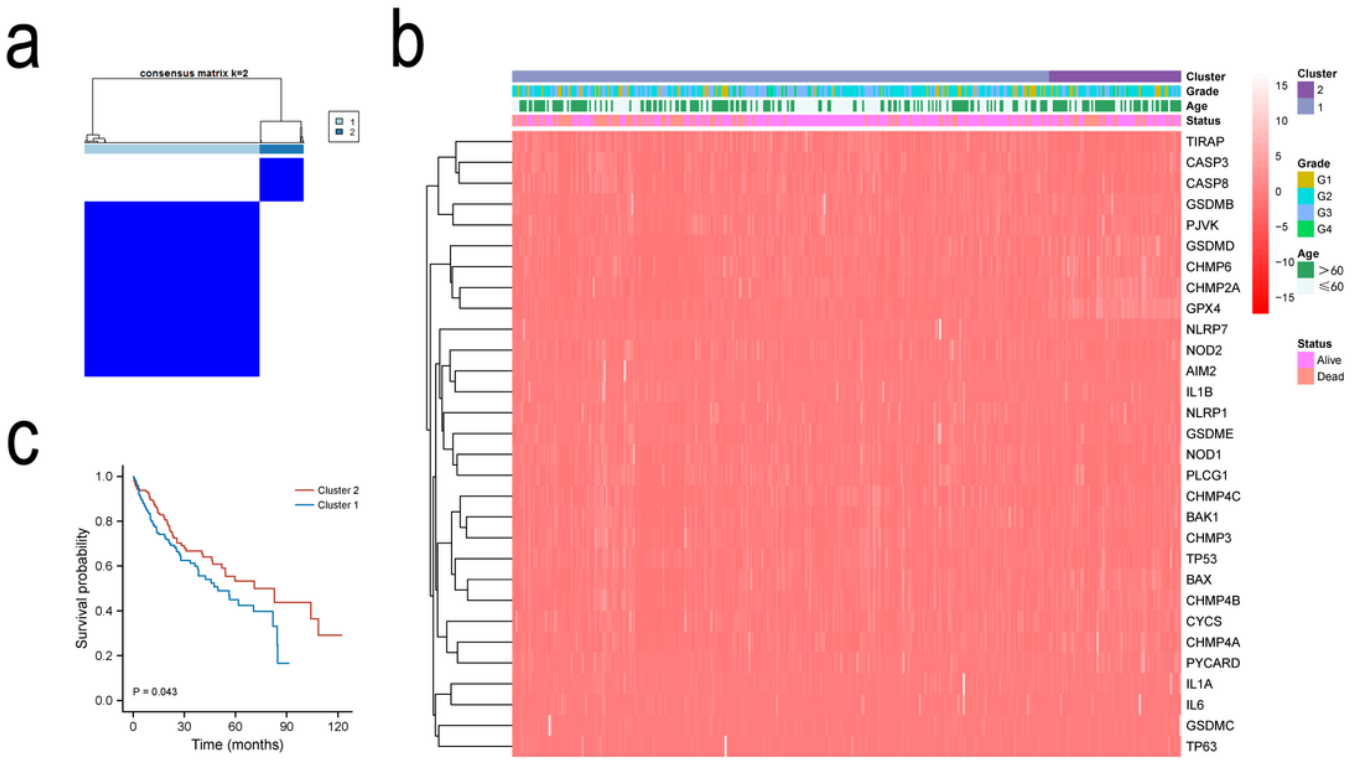

Figure 7

Tumour classification based on the pyroptosis-related DEGs a. HCC patients were grouped into 2 clusters according to the consensus clustering matrix (k = 2). b. Heatmap and the clinicopathologic characters of the 2 clusters classified by these DEGs c. C Kaplan–Meier OS curves for the 2 clusters.

Figure 8

Functional analysis based on the DEGs between the two-risk groups in the TCGA cohort a. Analysis of GO enrichment for DEGs.b. Analysis of KEGG enrichment for DEGs.

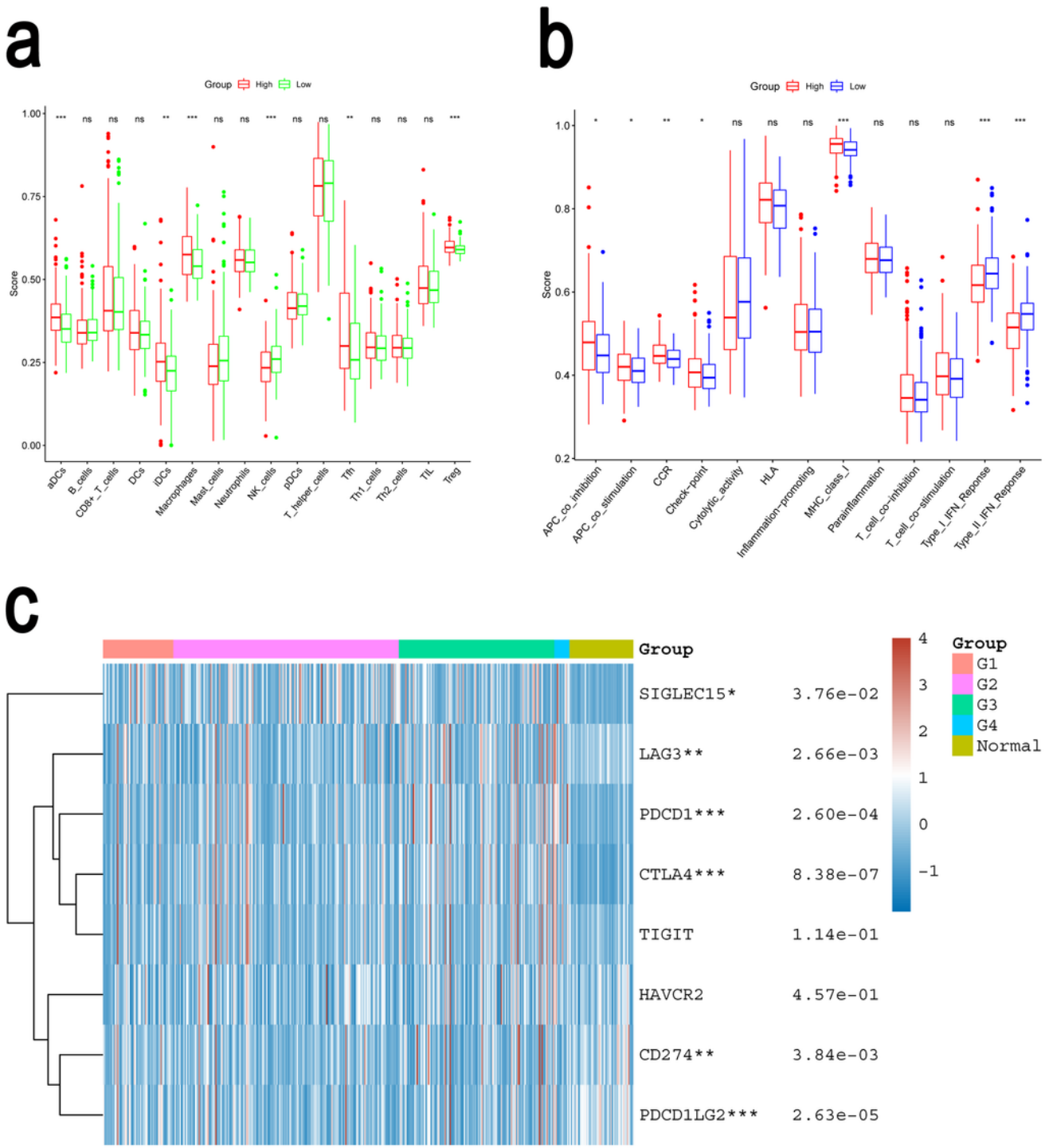

Figure 9

Comparison of the ssGSEA scores between different risk groups in the derivation cohort. The scores of 16 immune cells (a) and 13 immune-related functions (b) are displayed in boxplots.